# A tri-trophic model for the biological control of *Meloidogyne javanica* by *Purpureocillium lilacinum*: stability analysis and a biocontrol threshold

**Danilo Vasconceilos dos Santos** [1], **Bruna Rodrigues Moreira** [1] **and José Feliciano Bernardes Neto** [1,2*]

[1] *Center of Excellence in Bioinputs (CEBIO), Federal Institute Goiano (Instituto Federal Goiano), Rua 88, nº 310, Setor Sul, Goiânia, GO, 74085-010, Brazil*
[2] *Department of Crop Science and Plant Protection (Departamento de Fitotecnia e Fitossanidade), Faculty of Agronomy and Animal Science (FAAZ), Federal University of Mato Grosso (Universidade Federal de Mato Grosso, UFMT), Av. Fernando Corrêa da Costa, nº 2367, Boa Esperança, Cuiabá, MT, 78060-900, Brazil*

* *Corresponding author. E-mail: joseneto_agronomia@hotmail.com.br*

**ABSTRACT.** This study presents the development and analysis of a mathematical model to simulate the biological control of *Meloidogyne javanica* by the nematophagous fungus *Purpureocillium lilacinum*. The model adapts the Lotka–Volterra predator–prey framework to represent tri-trophic interactions among the host plant, J2, reproductive females, and the fungus. The system of ordinary differential equations was parameterized with literature-derived and exploratory values, non-dimensionalized, analyzed through Jacobian-based stability (Routh–Hurwitz criteria) and bifurcation analysis, and solved numerically in Python with the fourth-order Runge–Kutta method. Without the fungus, the nematode–plant system was unstable in most of the plausible parameter space and exhibited boom-and-bust oscillations with recurrent collapse of root mass. Inoculation of *P. lilacinum* at planting reduced the peaks of J2 and reproductive females by 61% and 65%, prevented root collapse, and drove the system to a stable coexistence equilibrium. The analysis yielded an explicit threshold for biocontrol, expressed through a fungal reproduction number and a critical attack rate at which the system undergoes a transcritical bifurcation. Attack rates just above this threshold mainly stabilized the system, whereas gains in root mass required higher attack intensities. Global sensitivity analysis indicated that, although nematode demographic parameters are the dominant determinants of root mass, the fungal attack rate is the main controllable driver of biocontrol performance. Because no greenhouse or field data were generated, these outputs should be interpreted as *in silico*, hypothesis-generating predictions that require empirical validation.

**Key words**: biocontrol agents, Lotka–Volterra model, nematode population dynamics, root-knot nematodes, stability analysis, tri-trophic modeling

**DOI**: https://doi.org/10.33837/msj.v9i2.1824

*Received: June 26th, 2026* *Accepted: November 9th, 2026* *Published: November 18th, 2026*
*Associate editor: Anderson Rodrigo da Silva*

## INTRODUCTION

Plant-parasitic nematodes are an increasing threat to agricultural production worldwide, infecting crops of major food, economic, and social importance (Jones et al., 2013). In Brazil, they cause high losses in commodities such as soybean, sugarcane, and coffee (Machado, 2014). Among them, the genus *Meloidogyne* is recognized for its extreme polyphagy and for causing some of the highest yield losses in global agriculture (Nicol et al., 2011; Jones et al., 2013). *Meloidogyne incognita*, *M. arenaria*, and *M. javanica* are among the most widely distributed and economically damaging root-knot nematode species, and *M. javanica* is particularly prevalent in tropical and subtropical regions (Hunt & Handoo, 2009; Elling, 2013).

As sedentary endoparasites, *Meloidogyne* spp. induce specialized feeding sites known as giant cells, which are hypertrophied, multinucleate cells derived from vascular parenchyma through repeated nuclear division without cytokinesis and which sustain the nematode throughout its life cycle (Williamson & Hussey, 1996). Feeding-site establishment is accompanied by gall formation, resulting from hyperplasia and hypertrophy of the surrounding cortical cells (Bird & Kaloshian, 2003). Adult females deposit their eggs in a gelatinous matrix that protects them against desiccation and soil antagonists (Orion & Kritzman, 1991), allowing populations to persist in the absence of a host and to disperse through soil and plant material (Jones et al., 2013).

Plant damage results from the cumulative effects of penetration, feeding-site establishment, and

*Copyright © The Author(s).*
*This is an open-access paper published by the Instituto Federal Goiano, Urutaí - GO, Brazil. All rights reserved. It is distributed under the terms of the Creative Commons Attribution 4.0 International License.*

reproduction, which redirect water, minerals, and photosynthates toward giant cells and impair root uptake and translocation (Bird & Kaloshian, 2003). The resulting reflex symptoms, including chlorosis, stunting, and flower or fruit abortion, often resemble nutrient deficiencies (Noling, 2016), and under high nematode densities or highly virulent populations plants may decline or die (Moens et al., 2009).

On a global scale, plant-parasitic nematodes cause annual yield losses estimated at approximately US$80 billion (Nicol et al., 2011). Chemical nematicides remain effective, but their use poses risks to environmental and human health, including soil and groundwater contamination (Desaeger et al., 2020). This reinforces the need for biologically based alternatives within integrated nematode management, such as resistant cultivars, cultural practices, and biological control agents, the latter increasingly incorporated into the category of bioinputs (Desaeger et al., 2020).

Although *Purpureocillium lilacinum* is widely recognized as an effective biocontrol agent against *Meloidogyne* spp., the quantitative and temporal dynamics of its interactions with the nematode and the host plant remain poorly characterized from a tri-trophic perspective. Previous mathematical approaches to fungal regulation of root-knot nematodes, such as the discrete *Pochonia*–nematode–root model of Ciancio et al. (2022), relied on numerically calibrated, parameter-rich formulations validated against empirical data, without deriving closed-form conditions for the stability of biological suppression. A continuous framework that admits analytical characterization of equilibria and their stability can complement such approaches by identifying explicit conditions under which a fungal antagonist establishes and protects the host.

In this context, the present study develops a tri-trophic model based on a Lotka–Volterra framework to represent interactions among the host plant, *M. javanica*, and *P. lilacinum*. The model is non-dimensionalized to identify the parameter groups that govern its behavior, and its equilibria are characterized analytically through Jacobian-based stability analysis, Routh–Hurwitz conditions, and bifurcation analysis. This treatment is used to (i) derive a threshold condition for fungal establishment, expressed as a fungal reproduction number and a critical attack rate, (ii) characterize the dynamics of the nematode–plant system with and without the fungus, and (iii) quantify the relative influence of nematode demographic and fungal parameters on root protection, providing a theoretical basis for the optimization of biological control strategies.

Because this study is theoretical and explores system behavior under explicit assumptions, no primary greenhouse or field data were generated. The model was parameterized with literature-derived values and analyzed to generate experimentally testable hypotheses, providing a quantitative framework to guide future empirical studies and model validation.

## MATERIAL AND METHODS

### Model formulation

The proposed model is a continuous tri-trophic system inspired by Lotka–Volterra predator–prey principles and adapted to describe nematode–fungus–plant interactions. The state variables are J(t), the density of second-stage juveniles (J2); N(t), the density of reproductive (egg-laying) females; F(t), the density of fungal propagules; and H(t), the fresh root mass of the host plant. N represents reproductive females rather than the total adult population because *M. javanica*, like the other tropical root-knot nematode species, reproduces by obligatory mitotic parthenogenesis (Castagnone-Sereno et al., 2013). Males are therefore not required for reproduction and do not maintain feeding sites (Moens et al., 2009). Accordingly, J2 recruitment ($bNH/K_H$) and root consumption ($cNH$) are both attributed to N, and g is the rate at which J2 become established reproductive females.

The host is treated as a generic annual plant rather than a specific crop. Root mass is expressed relative to its carrying capacity $K_H$, which is set to 1000 as a normalization unit rather than a measured value. The system of ordinary differential equations is:

$$dJ/dt = b\,N\,(H/K_H) - (g + u_J + a\,F)\,J,$$
$$dN/dt = g\,J - u_N\,N,$$
$$dF/dt = e\,a\,J\,F - u_F\,F,$$
$$dH/dt = r_H\,H\,(1 - H/K_H) - c\,N\,H.$$

J2 recruitment is proportional to available root mass, representing the dependence of reproduction on host resources. The fungal growth term ($e \cdot a \cdot J \cdot F$) assumes that the increase of *P. lilacinum* results from parasitic activity on nematodes (Khan & Tanaka, 2023). Here, a is the attack rate (per capita rate at which J2 are infected per unit of fungal propagule density), and e is the conversion efficiency of parasitized J2 into new fungal propagules. *P. lilacinum* also parasitizes eggs and egg-laying females and can grow saprophytically in soil. The model represents these processes implicitly through a single parasitic interaction with the mobile J2 stage. This simplification isolates the component of fungal activity that directly couples antagonist and pest dynamics and keeps the system analytically tractable.

**Table 1.** Parameters of the tri-trophic model among the host plant, *Meloidogyne javanica*, and *Purpureocillium lilacinum*: baseline values used in all simulations and ranges explored in the global sensitivity analysis.

| Parameter | Description | Unit | Baseline | Range | Source |
|---|---|---|---|---|---|
| b | J2 recruitment rate per reproductive female | J2 female$^{-1}$ day$^{-1}$ | 0.60 | 0.3–0.8 | Gupta et al. (2018)[a] |
| g | Transition rate from J2 to reproductive female | day$^{-1}$ | 0.10 | 0.07–0.12 | Ploeg & Maris (1999)[a] |
| $u_J$ | J2 natural mortality | day$^{-1}$ | 0.03 | 0.01–0.05 | Lu et al. (2022)[a] |
| $u_N$ | Reproductive female natural mortality | day$^{-1}$ | 0.04 | 0.03–0.05 | Ciancio et al. (2022) |
| $u_F$ | Fungal propagule mortality | day$^{-1}$ | 0.04 | 0.03–0.06 | Parajuli et al. (2014) |
| a | Fungal attack rate on J2 | day$^{-1}$ (propagule density)$^{-1}$ | 0.005 | 0.001–0.010 | Assumed[b] |
| e | Conversion efficiency of parasitized J2 into fungal propagules | propagule J2$^{-1}$ | 0.90 | 0.8–1.0 | Assumed[b] |
| $r_H$ | Intrinsic root growth rate | day$^{-1}$ | 0.05 | 0.02–0.06 | Assumed[b] |
| c | Root consumption rate by reproductive females | day$^{-1}$ female$^{-1}$ | 0.002 | 0.001–0.010 | Scaling coefficient[c] |
| $K_H$ | Root carrying capacity | relative units | 1000 | Fixed | Model normalization[d] |

[a] Values based on studies with *Meloidogyne incognita*, used as a proxy for *M. javanica*. [b] Exploratory value assigned within a plausible range in the absence of direct empirical estimates; influence evaluated in the global sensitivity analysis. [c] Fixed to produce a marked decline in root mass during the first nematode generation in fungus-free simulations; enters the dynamics only through the composite group $\kappa = ea/c$. [d]Normalization unit for root mass ($H_0 = K_H$), not a measured value. Initial conditions: $J_0 = 10$, $N_0 = 5$, $H_0 = 1000$; $F_0 = 0$ (fungus-free scenario) or $F_0 = 10$ (inoculation at planting). Ranges were sampled by Latin hypercube (n = 1000).

**Parameterization**

Baseline values and ranges are summarized in Table 1, and all simulations used the same baseline set:

$b = 0.6$, $g = 0.1$, $u_J = 0.03$, $u_N = 0.04$, $u_F = 0.04$, $a = 0.005$, $e = 0.9$, $r_H = 0.05$, $c = 0.002$, and $K_H = 1000$.

Nematode demographic parameters (b, g, $u_J$, $u_N$) and fungal mortality ($u_F$) were set within ranges consistent with published life-history and population studies (Table 1). Because comparable data for *M. javanica* are scarce, the reproduction and development parameters were based on studies with *M. incognita*, a closely related tropical species with a similar life cycle.

Parameters without direct empirical estimates (a, e, $r_H$, and c) were assigned exploratory values within plausible ranges. Their influence on model outputs was evaluated in the global sensitivity analysis.

Parameter c has no direct empirical counterpart, because the model does not resolve the physiological mechanisms of root damage. It was therefore treated as a scaling coefficient and fixed at a value that produces a marked decline in root mass during the first nematode generation in fungus-free simulations. As shown in the non-dimensional analysis below, c only sets the density scale of the nematode variables and enters the dynamics through the composite group $\kappa = ea/c$.

Similarly, e was assigned values between 0.8 and 1.0 propagule units per parasitized J2 under the model normalization. Because e enters the dynamics only through $\kappa$, its value rescales the effective attack rate rather than altering the qualitative behavior of the system.

**Numerical solution**

All simulations used the original (dimensional) system. The dimensionless form below was used only for analytical results. The system was solved in Python (NumPy) with the classical fourth-order Runge–Kutta method and a fixed step of 0.1 day. Initial conditions were $J_0 = 10$, $N_0 = 5$, and $H_0 = K_H = 1000$ in all scenarios. The fungus-free scenario used $F_0 = 0$, and the biocontrol scenario used $F_0 = 10$, representing a single inoculation at planting ($t = 0$). This is consistent with the use of *P. lilacinum* strain 251 as a soil treatment at planting that sustains nematode suppression through the growing season (Dahlin et al., 2019). Both scenarios share all parameter values and initial nematode and host densities and differ only in the fungal inoculum.

Simulations were run for 250 days, a horizon representative of an annual host cycle that covers several nematode generations. Because the fungus-free system may oscillate rather than settle at equilibrium (see Results), two output measures were used:

1. root mass at the end of the 250-day horizon (H at day 250);
2. the long-run mean root mass, computed as the mean of H over the last 1000 days of a 4000-day simulation.

In field applications, the dose of fungal bioinputs refers to the amount of product per unit area (e.g., g ha$^{-1}$ or L ha$^{-1}$). In population models, application intensity is instead represented by the initial density of the biocontrol agent under a chosen normalization. $F_0$ was therefore interpreted as a proxy for inoculum pressure in model units rather than as a direct conversion of a commercial dose. The Python code that

reproduces all simulations and figures is provided as Supplementary Material.

**Non-dimensionalization**

To reduce the number of independent parameters and identify the groups that govern system behavior, the model was rescaled with:

$j = (c/g)\, J$, $n = (c/g)\, N$, $\varphi = (a/g)\, F$, $h = H/K_H$, $\tau = g\, t$.

Substitution into the original system yields:

$$dj/d\tau = \beta\, n\, h - (1 + \mu_J + \varphi)\, j,$$
$$dn/d\tau = j - \mu_N\, n,$$
$$d\varphi/d\tau = (\kappa\, j - \mu_F)\, \varphi,$$
$$dh/d\tau = \rho\, h\, (1 - h) - n\, h,$$

where the dimensionless parameter groups are:

$$\beta = b/g,\ \mu_J = u_J/g,\ \mu_N = u_N/g,$$
$$\mu_F = u_F/g,\ \rho = r_H/g,\ \kappa = e\, a/c.$$

This transformation reduces the ten-dimensional parameters to six dimensionless groups. It absorbs $K_H$ into h and the root consumption rate c into the scale of the nematode variables. It remains valid for $a = 0$, which corresponds to $\kappa = 0$ and $\varphi \equiv 0$, that is, absence of fungal action. The attack rate (a) and the conversion efficiency (e) enter only through $\kappa = ea/c$, so the two parameters act jointly through the effective intensity of the fungus–nematode interaction and are not separately identifiable from the qualitative behavior of the system.

**Existence, positivity, and well-posedness**

The right-hand sides of the system are polynomial in the state variables and therefore locally Lipschitz. This ensures existence and uniqueness of solutions and continuous dependence on initial conditions over finite time intervals. The nonnegative orthant is forward invariant: whenever a state variable reaches zero, its time derivative is nonnegative, so no variable becomes negative.

**Equilibria**

Setting the dimensionless system to steady state yields four biologically meaningful equilibria:

1. $E_0 = (0, 0, 0, 0)$: total collapse;
2. $E_1 = (0, 0, 0, 1)$: healthy, nematode-free plant at its carrying capacity;
3. $E_2$: fungus-free nematode–plant equilibrium;
4. $E_3$: coexistence equilibrium with active biocontrol.

The non-trivial equilibria are:

$E_2$: $h_2 = \mu_N\, (1 + \mu_J)/\beta$, $n_2 = \rho\, (1 - h_2)$, $j_2 = \mu_N\, n_2$, $\varphi_2 = 0$;
$E_3$: $j_3 = \mu_F/\kappa$, $n_3 = j_3/\mu_N$, $h_3 = 1 - n_3/\rho$, $\varphi_3 = \beta\, h_3/\mu_N - (1 + \mu_J)$.

$E_2$ is admissible when $h_2 < 1$, that is, when the nematode reproduction number $R_N = \beta/[\mu_N\, (1 + \mu_J)]$ exceeds unity. $E_3$ is admissible when $\varphi_3 > 0$. Because $\varphi_3 > 0$ is equivalent to $h_3 > h_2$, $j_3 < j_2$, and $\kappa\, j_2 > \mu_F$, the coexistence equilibrium exists exactly when the fungus can invade the fungus-free equilibrium. Whenever it exists, it necessarily has lower J2 and female densities and higher root mass than $E_2$.

**Local stability and the biocontrol threshold**

The Jacobian matrix of the dimensionless system at a generic point (j, n, φ, h), with rows corresponding to the j, n, φ, and h equations, is:

$$\text{Row j: } [\, -(1 + \mu_J + \varphi),\ \beta\, h,\ -j,\ \beta\, n\, ]$$
$$\text{Row n: } [\, 1,\ -\mu_N,\ 0,\ 0\, ]$$
$$\text{Row } \varphi\text{: } [\, \kappa\, \varphi,\ 0,\ \kappa\, j - \mu_F,\ 0\, ]$$
$$\text{Row h: } [\, 0,\ -h,\ 0,\ \rho\, (1 - 2h) - n\, ]$$

$E_0$ is always unstable, because the root equation contributes the positive eigenvalue ρ. At $E_1$, the eigenvalues are $-\mu_F$, $-\rho$, and the two eigenvalues of the juvenile–female block, which are both negative if and only if $R_N < 1$. $E_1$ is therefore stable only when the nematode cannot invade the healthy plant.

**Stability of $E_2$**

At $E_2$, the Jacobian is block triangular with respect to the fungal direction. One eigenvalue equals $\kappa\, j_2 - \mu_F$, and the remaining three are the roots of the characteristic polynomial of the nematode–plant subsystem:

$$P_2(\lambda) = \lambda^3 + a_1\lambda^2 + a_2\lambda + a_3,$$
$$a_1 = 1 + \mu_J + \mu_N + \rho\, h_2,$$
$$a_2 = \rho\, h_2\, (1 + \mu_J + \mu_N),$$
$$a_3 = \mu_N\, (1 + \mu_J)\, \rho\, (1 - h_2).$$

All coefficients are positive whenever $E_2$ is admissible ($0 < h_2 < 1$). By the Routh–Hurwitz criterion, the subsystem is therefore locally asymptotically stable if and only if $a_1 a_2 > a_3$, that is:

$$h_2\, (1 + \mu_J + \mu_N)(1 + \mu_J + \mu_N + \rho\, h_2) > \mu_N\, (1 + \mu_J)(1 - h_2).$$

This condition is not guaranteed in the admissible domain. It holds for low nematode reproduction ($h_2$ close to 1) but fails when $R_N$ is large. When $a_1 a_2 < a_3$, a pair of complex eigenvalues has positive real part, $E_2$ loses stability through a Hopf bifurcation, and the fungus-free system exhibits sustained oscillations. The condition was evaluated at the baseline values and across the ranges in Table 1.

**Biocontrol threshold**

The fungal eigenvalue at $E_2$ is positive if and only if $\kappa\, j_2 > \mu_F$. In the original variables, this condition

defines the fungal (biocontrol) reproduction number and the corresponding critical attack rate:

$R_N = b\, g/[u_N\,(g + u_J)]$,
$R_F = e\, a\, J_2^*/u_F$,
$a_{crit} = u_F/(e\, J_2^*)$,

where $J_2^* = u_N\, r_H\,(1 - 1/R_N)/(g\, c)$ is the J2 density at the fungus-free equilibrium and does not depend on a or e. The fungus establishes and the coexistence equilibrium $E_3$ exists if and only if $R_F > 1$, equivalently $a > a_{crit}$. When $E_2$ is unstable and the fungus-free system oscillates, this criterion is a local approximation of the invasion condition. The threshold was therefore also verified numerically (see Results).

**Stability of $E_3$**

At $E_3$, the characteristic polynomial of the Jacobian is:

$P_3(\lambda) = \lambda^4 + c_1\lambda^3 + c_2\lambda^2 + c_3\lambda + c_4$,
$c_1 = \rho\, h_3 + \mu_N + D$,
$c_2 = \rho\, h_3\,(\mu_N + D) + \mu_F\, \varphi_3$,
$c_3 = \mu_F\, \varphi_3\,(\mu_N + \rho\, h_3) + \beta\, \rho\, h_3\,(1 - h_3)$,
$c_4 = \mu_F\, \mu_N\, \rho\, \varphi_3\, h_3$,

with $D = 1 + \mu_J + \varphi_3 = \beta\, h_3/\mu_N$. All coefficients are positive when $E_3$ is admissible. By the Routh–Hurwitz criterion for quartic polynomials, $E_3$ is locally asymptotically stable if and only if:

$$c_1c_2 - c_3 > 0 \text{ and } c_1c_2c_3 - c_3^2 - c_1^2c_4 > 0.$$

These conditions were evaluated at the baseline values, along the attack-rate gradient, and across the parameter ranges in Table 1. The criteria were confirmed by direct computation of the Jacobian eigenvalues. Stability across the parameter space was assessed for 20 000 parameter sets drawn uniformly from the ranges in Table 1.

**Bifurcation behavior**

$R_F$ increases linearly with the attack rate a. As a increases through $a_{crit}$ ($R_F = 1$), $\varphi_3$ and $c_4$ vanish, $E_3$ coincides with $E_2$, and one eigenvalue crosses zero. This defines a transcritical bifurcation in which the fungus-free state loses stability in the fungal direction and the coexistence equilibrium becomes admissible. Above the threshold, $h_3$ increases monotonically with a, so the equilibrium root mass rises with attack intensity.

The bifurcation was examined numerically by varying a from 0 to 0.010 with all other parameters at baseline. For each value, the long-run mean root mass and the root mass at day 250 were compared with the analytical equilibria $H_2 = K_H\, h_2$ and $H_3 = K_H\, h_3$. A two-parameter analysis was also performed by varying a (0 to 0.010) and the nematode reproduction rate b (0.3 to 0.8, the range in Table 1). This analysis recorded root mass at day 250 and overlaid the analytical threshold $a_{crit}(b)$.

**Sensitivity analysis**

A global sensitivity analysis was performed to assess the robustness of model predictions to parameter uncertainty. One thousand parameter sets were generated by Latin hypercube sampling over the ranges in Table 1, and the system was simulated for each set under the biocontrol scenario. Partial rank correlation coefficients (PRCC) were computed between each parameter and root mass at day 250. Significance was assessed by a t-test ($\alpha = 0.05$). PRCC values for the long-run mean root mass were also computed to verify the consistency of the ranking. This global approach complements the local stability analysis by quantifying the relative influence of each parameter across the plausible parameter space rather than around a single operating point.

## RESULTS AND DISCUSSION

**Population dynamics with and without the fungus**

In the absence of *P. lilacinum*, the simulated dynamics of *M. javanica* followed the pattern expected for an unmanaged infestation (Figure 1a). J2 density increased rapidly and peaked at 115 individuals on day 23. The density of reproductive females (N) peaked shortly thereafter, at 148 individuals on day 34, reflecting the interval between J2 establishment and female maturation. The increase in nematode densities was accompanied by a sharp decline in root fresh mass (H), which fell below 10% of its initial value by day 27 and remained close to zero between days 50 and 220. As root tissue became scarce, J2 recruitment declined and both nematode stages decreased to near-zero densities. Root mass then began to recover and reached 42 at day 250.

Inoculation with *P. lilacinum* at planting substantially altered these dynamics (Figure 1b). The peaks of J2 and reproductive females were reduced by 61% and 65%, respectively, relative to the fungus-free scenario (45 J2 on day 16 and 52 females on day 25). The fungal population increased rapidly, peaked at 124 on day 33, after the J2 peak, and then declined without disappearing. Root mass declined to a minimum of 111 on day 61, an order of magnitude above the fungus-free minimum, and remained between 110 and 270 for the rest of the simulation, reaching 183 at day 250. Nematode, fungal, and root densities showed damped oscillations of decreasing amplitude over the simulation period. These values are model predictions under the stated assumptions, not empirical measurements.

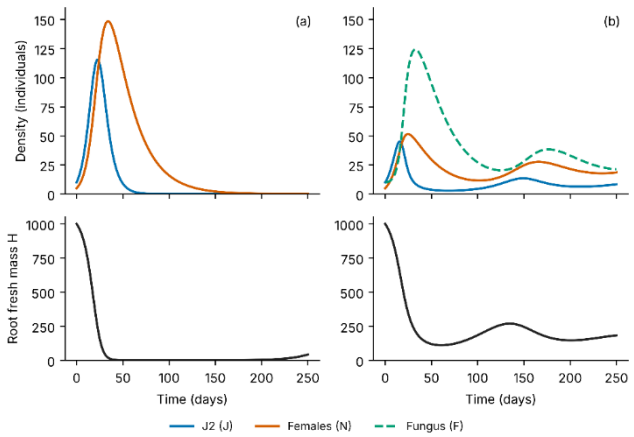



**Figure 1.** Simulated dynamics of second-stage juveniles (J2, J), reproductive females (N), fungal propagules (F), and host root fresh mass (H) over 250 days. (a) Fungus-free scenario ($F_0 = 0$). (b) Biocontrol scenario with *Purpureocillium lilacinum* inoculated at planting ($F_0 = 10$; attack rate a = 0.005). Both scenarios share all parameter values and initial conditions ($J_0 = 10$, $N_0 = 5$, $H_0 = 1000$; Table 1). Upper panels show nematode and fungal densities, and lower panels show root fresh mass in relative units ($K_H = 1000$).

## Stability of the equilibria and the biocontrol threshold

At baseline values, the nematode reproduction number was $R_N = 11.5$, so the fungus-free equilibrium $E_2$ was admissible ($H_2 = 86.7$). However, its Routh–Hurwitz condition was violated ($a_1a_2 - a_3 = -0.109$), and $E_2$ had a pair of complex eigenvalues with positive real part ($0.017 \pm 0.365i$). The fungus-free system therefore does not settle at equilibrium. It converges to sustained oscillations, with a period of about 275 days, in which root mass alternates between near-collapse (minimum 0.6) and recovery (maximum 605). Across 20 000 parameter sets drawn uniformly from the ranges in Table 1, $R_N$ was always greater than one and $E_2$ was stable in only 12% of the sets. Instability of the fungus-free state is therefore the typical behavior of the nematode–plant subsystem within the plausible parameter space.

The critical attack rate at baseline was $a_{crit} = 0.0049$. The baseline attack rate (a = 0.005) lies just above this threshold ($R_F = 1.03$), so the fungus establishes and the system approaches the coexistence equilibrium $E_3$ (J = 8.9, N = 22.2, F = 7.3, H = 111.1). Both Routh–Hurwitz conditions for $E_3$ were satisfied ($c_1c_2 - c_3 = 0.19$; $c_1c_2c_3 - c_3^2 - c_1^2c_4 = 0.055$). Its eigenvalues were $-2.080$, $-0.017 \pm 0.416i$, and $-0.009$, so the approach to $E_3$ consists of damped oscillations, with a period of about 150 days, and a slow final convergence. This explains why oscillations persisted throughout the 250-day simulation (Figure 1b). The stability margins increased with the attack rate (for example, $c_1c_2 - c_3 = 25.0$ and $c_1c_2c_3 - c_3^2 - c_1^2c_4 = 41.8$ at a = 0.008). Across the parameter sets in which $E_3$ was admissible, it was stable in 98% of cases.

The bifurcation diagram confirmed the analytical threshold (Figure 2). For a above $a_{crit}$, both the long-run mean root mass and the root mass at day 250 coincided with the analytical equilibrium $H_3$, which increased monotonically with the attack rate ($H_3 = 259$ at a = 0.006, 444 at a = 0.008, and 556 at a = 0.010). For a below $a_{crit}$, the fungus did not persist. The long-run mean root mass then reflected the fungus-free oscillations (107 to 140) rather than the unstable equilibrium $H_2$. Root mass at day 250 varied irregularly with a (1 to 545), because it depended on the phase of the nematode–root oscillation at the end of the simulation rather than on stable protection. In numerical simulations, the fungus persisted from a ≈ 0.0048, in close agreement with the analytical value, given that the criterion is evaluated at an unstable equilibrium.

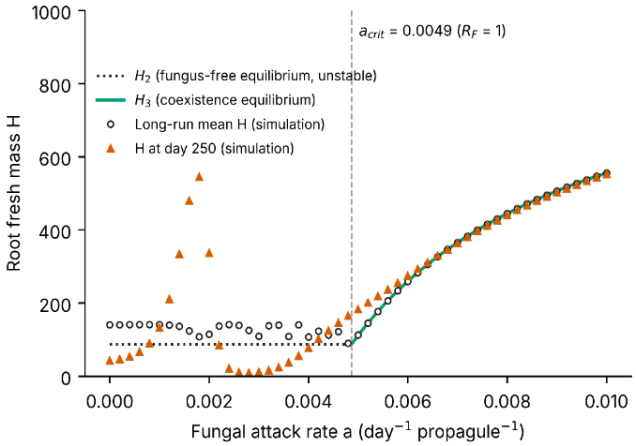



**Figure 2.** Bifurcation diagram of host root fresh mass (H) as a function of the fungal attack rate (a), with all other parameters at baseline. Dotted line: fungus-free equilibrium $H_2$ (unstable at baseline). Solid line: analytical coexistence equilibrium $H_3$, admissible for $a > a_{crit}$. Circles: long-run mean root mass (mean over days 3000–4000). Triangles: root mass at day 250. The dashed vertical line marks the critical attack rate $a_{crit} = 0.0049$, at which the fungal reproduction number $R_F$ equals 1 (transcritical bifurcation). All simulations used the original (dimensional) system.

At the baseline attack rate, which lies close to the threshold, the main effect of the fungus was to stabilize the system rather than to raise long-run root mass. The coexistence equilibrium ($H_3 = 111$) was comparable to the long-run mean of the fungus-free oscillations (140) but eliminated their recurrent root collapses. Root protection beyond this stabilizing effect required attack rates moderately above $a_{crit}$ ($H_3 > 140$ for $a \geq 0.0054$).

## Two-parameter analysis

The two-parameter analysis showed that the threshold $a_{crit}(b)$ varied little across the range of b (from 0.0054 at b = 0.3 to 0.0048 at b = 0.8) and separated two qualitatively different regions (Figure 3). Above the threshold, root mass at day 250 increased consistently with a and was nearly independent of b (about 550 at a = 0.010 for all values of b). Below the threshold, root mass at day 250 depended strongly on b and on the timing of the nematode–root oscillation. With a = 0, it ranged from 401 at b = 0.3 to near zero at b = 0.8. The

high-root-mass regions at low a therefore reflect scenarios of intrinsically low nematode pressure, or the end of the simulation coinciding with a phase of root recovery, rather than effective fungal control.

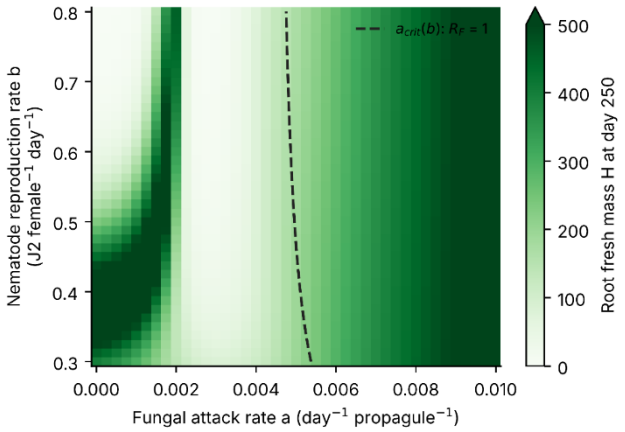



**Figure 3.** Root fresh mass (H) at day 250 as a function of the fungal attack rate (a, 0–0.010) and the nematode reproduction rate (b, 0.3–0.8, the range in Table 1), with all other parameters at baseline. Darker shading indicates higher root mass, and values above 500 are shown in the darkest shade. The dashed line shows the analytical threshold $a_{crit}(b)$, at which $R_F = 1$.

### Phase-space dynamics

Phase portraits of the baseline biocontrol scenario illustrated the convergence of the system toward the coexistence equilibrium (Figure 4). In both the fungus–J2 projection (Figure 4a) and the female–root projection (Figure 4b), trajectories performed an initial large excursion, associated with the first nematode generation and fungal proliferation, followed by spirals of decreasing amplitude around $E_3$. This is consistent with the complex eigenvalues with negative real parts obtained analytically. At day 2500, the state variables were within 1% (J, N) to 12% (F) of their equilibrium values.

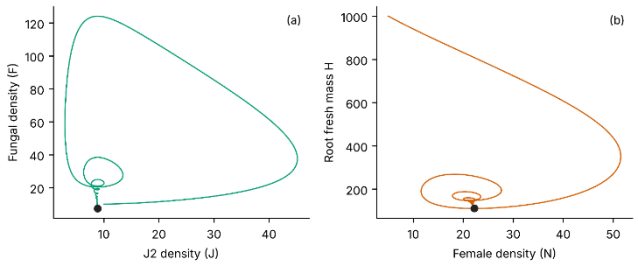



**Figure 4.** Phase portraits of the baseline biocontrol scenario (a = 0.005; $F_0$ = 10 at planting) simulated over 2500 days. (a) Fungal propagules (F) versus second-stage juveniles (J). (b) Root fresh mass (H) versus reproductive females (N). Black dots mark the coexistence equilibrium $E_3$. Trajectories spiral with decreasing amplitude toward $E_3$, consistent with its local asymptotic stability.

### Global sensitivity analysis

Global sensitivity analysis quantified the relative influence of each parameter on root mass at day 250 (Figure 5). The nematode reproduction rate (b, PRCC = −0.31) and the root consumption rate (c, −0.25) had the strongest negative effects, followed by female mortality ($u_N$, +0.19). Among the parameters of the biocontrol agent, the attack rate (a, +0.15) was the most influential. It exceeded fungal mortality ($u_F$, −0.09), whereas conversion efficiency (e) had no significant effect (PRCC = −0.002, p = 0.95). The remaining parameters (g, $u_J$, $r_H$) had smaller but significant effects ($|PRCC| \leq 0.13$; $p < 0.05$). The signs of all significant correlations were biologically consistent: higher nematode reproduction and consumption reduced root mass, whereas higher female mortality and higher attack rate increased it.

The same ranking of fungal parameters was obtained for long-run root mass. Nematode demographic parameters had larger coefficients for this output (b, −0.58; $u_N$, +0.63; g, −0.36), and the attack rate remained the most influential fungal parameter (a, +0.11; $u_F$, −0.12, with comparable magnitudes; e not significant). Because the nematode demographic parameters are intrinsic properties of the pest population and are not subject to management, the attack rate emerges as the principal controllable determinant of biocontrol performance, consistent with the threshold identified analytically.

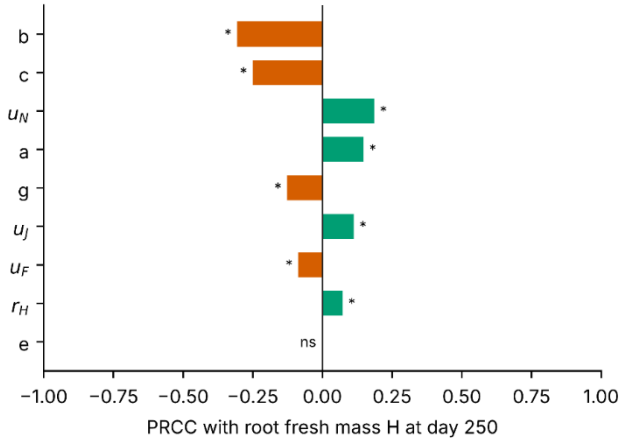



**Figure 5.** Global sensitivity analysis of root fresh mass (H) at day 250. Bars show partial rank correlation coefficients (PRCC) between each parameter and H, computed from 1000 parameter sets generated by Latin hypercube sampling over the ranges in Table 1 under the biocontrol scenario. Green bars indicate parameters that increase root mass, and orange bars indicate parameters that decrease it. *, $p < 0.05$; ns, not significant (t-test).

## DISCUSSION

Given the theoretical nature of this work, the results should be interpreted as exploratory predictions derived from model structure rather than as empirical observations. Under the model assumptions, inoculation of *P. lilacinum* at planting reduced the peaks of J2 and reproductive females by 61% and 65%, respectively, and prevented the near-complete loss of root mass observed in the fungus-free scenario. Complete suppression of the nematode was not achieved. Instead, the system converged to a

coexistence state in which nematode densities were lower and root mass was maintained. These predictions are qualitatively consistent with greenhouse and field studies. On tomato, *P. lilacinum* reduced galls by 74%, egg masses by 71%, and soil J2 by 59% relative to untreated plants (El-Ashry et al., 2021). In field-grown carrot, it was effective enough to be recommended as an alternative to chemical nematicides (Santos & Martinelli, 2022). The model does not include an explicit damage threshold relating nematode density to yield loss. Its predictions should therefore be read as reductions in nematode density and gains in root mass and stability relative to the fungus-free scenario, not as maintenance of populations below economic damage levels.

A central contribution of this study is the analytical derivation of a threshold condition for biocontrol. The fungus establishes only when its reproduction number, $R_F = e \cdot a \cdot J_2^*/u_F$, exceeds unity, equivalently when the attack rate exceeds $a_{crit} = u_F/(e \cdot J_2^*)$. At that point, the system undergoes a transcritical bifurcation from the fungus-free state to the coexistence equilibrium. Because the coexistence equilibrium exists exactly when $R_F > 1$ and always has higher root mass than the fungus-free equilibrium, the threshold separates biocontrol failure from biocontrol success in a single, interpretable condition. The numerical simulations confirmed this prediction: fungal persistence began at an attack rate close to the analytical value, and root mass above the threshold followed the analytical equilibrium. The threshold also depends on $J_2^*$, the J2 density sustained by the host in the absence of the fungus. Conditions that increase $J_2^*$ lower $a_{crit}$, which means that a fungus whose growth depends on parasitism establishes more easily where nematode pressure is high.

The stability analysis revealed a second, less evident result. Without the fungus, the nematode–plant subsystem was unstable in most of the plausible parameter space, including the baseline. Instead of settling at equilibrium, it entered sustained boom-and-bust oscillations, with recurrent near-collapse of root mass. The coexistence equilibrium, in contrast, was stable in almost all cases in which it existed. The fungus therefore acts not only by reducing nematode densities but also by converting an oscillatory host–parasite system into a stable one. This distinction matters for interpretation. At the baseline attack rate, which lies just above $a_{crit}$, the long-run root mass under biocontrol was comparable to the long-run mean of the fungus-free oscillations, and the benefit of the fungus consisted mainly of eliminating root collapses. Gains in long-run root mass required attack rates moderately above the threshold, beyond which equilibrium root mass increased steadily with a. Successful biocontrol therefore requires attack intensity sufficiently above the threshold, not merely fungal persistence.

Global sensitivity analysis refined this interpretation. Across the parameter space, root mass was governed most strongly by nematode reproduction, root consumption, and female mortality. These are intrinsic properties of the pest–host interaction and are not subject to direct management. Among the parameters of the biocontrol agent, the attack rate was the most influential, followed by fungal mortality, whereas conversion efficiency had no significant effect. This is consistent with the non-dimensional analysis, in which a and e act jointly through $\kappa = ea/c$, and with the threshold condition, in which a and $u_F$ appear directly. The attack rate therefore emerges as the principal controllable determinant of biocontrol performance, even though it is not the dominant driver of system behavior in absolute terms. This identifies the attack rate, together with fungal persistence in soil, as the targets most amenable to optimization through strain selection, inoculum quality, and application strategy.

The proposed framework provides a computational approach to explore the dynamics of tri-trophic interactions among host plants, nematodes, and fungal antagonists. Although such approaches remain relatively underexplored in nematology, they can integrate biological knowledge, generate testable hypotheses, and support decision-making in integrated pest management. The modified Lotka–Volterra structure captured essential ecological behaviors: host–parasite oscillations arising through a Hopf bifurcation, an invasion threshold for the antagonist formalized as a transcritical bifurcation, and convergence to a stable coexistence equilibrium through damped oscillations. It may be adapted to other nematode–antagonist systems.

From an applied perspective, the results suggest that biocontrol success depends on conditions that keep the effective attack rate above the critical value, such as adequate inoculum density, environmental conditions favorable to fungal activity, and fungal persistence in soil. Because the baseline attack rate lies close to the threshold, moderate reductions in fungal activity could shift the system from stable control to failure. The timing and frequency of application were not evaluated here and represent a natural extension of the model.

The model has several limitations. It assumes a homogeneous environment and does not account for spatial heterogeneity, soil texture, microsite variability, or host genetic factors that influence nematode infection success and fungal performance (Williamson & Hussey, 1996; Jones et al., 2013). Parasitism of eggs and egg-laying females, a major mode of action of *P. lilacinum*, is represented only implicitly through the interaction with J2. The attack rate, conversion efficiency, root growth rate, and root consumption rate lack direct empirical estimates, and part of the nematode parameters were based on *M. incognita*. The model is deterministic. Environmental variability such as rainfall

pulses, temperature fluctuations, and soil disturbance may temporarily reduce the effective attack rate and allow transient nematode rebounds. Below the threshold, root mass at a fixed date depends on the phase of the nematode–root oscillation, so end-of-season values in that regime should not be interpreted as protection. Consequently, model predictions should be interpreted as qualitative expectations rather than precise forecasts.

Future extensions may incorporate stochastic or environment-dependent parameters to improve predictive reliability under field conditions. Treating key parameters as time-dependent or environmentally driven, for example a(t) or a(T, θ, pH), would allow estimation of confidence bands around trajectories and of the probability of control failure. An explicit egg stage would allow egg parasitism to be represented directly. Coupling root mass or nematode density to a damage function, such as the Seinhorst model (Seinhorst, 1965), would translate the predictions into yield losses and economic thresholds. Interactions with other soil microorganisms, competitive saprophytes, and additional antagonists could also be incorporated.

Model predictions can be tested in greenhouse or field trials by monitoring over time: (i) J2 density in rhizosphere soil, corresponding to J(t); (ii) colony-forming units of *P. lilacinum* in soil and roots, corresponding to F(t); (iii) the number of egg-laying females or egg masses per root system, corresponding to N(t); (iv) root fresh mass, corresponding to H(t); and (v) the prevalence of parasitized eggs and egg masses as an indicator of fungal activity. Such time series would allow the parameters to be estimated, $a_{crit}$ to be calculated empirically, and the predicted threshold behavior to be tested.

Overall, the findings provide a theoretical basis for the optimization of biological control strategies and support computational modeling as a complementary tool for understanding and improving sustainable nematode management.

## CONCLUSION

This study indicates, based on *in silico* simulations, that *P. lilacinum* may alter the population dynamics of *M. javanica* by reducing the peaks of second-stage juveniles and reproductive females and by preventing the collapse of host root mass under the model assumptions. The tri-trophic model, based on modified Lotka–Volterra equations, suggests that the fungus acts primarily as a regulatory agent. It lowers nematode densities and converts an oscillatory, collapse-prone nematode–plant system into a stable coexistence state, rather than eradicating the nematode.

A central outcome of the model was the analytical identification of a threshold for biocontrol success, expressed through the fungal reproduction number $R_F$ and a corresponding critical attack rate. At this threshold, the system undergoes a transcritical bifurcation from the fungus-free state to a coexistence equilibrium, which was locally stable in almost all parameter combinations in which it existed. Attack rates just above the threshold mainly stabilized the system, whereas gains in root mass required attack rates moderately above it. Below the threshold, the fungus did not persist. Global sensitivity analysis indicated that, although nematode demographic parameters are the dominant determinants of root mass, the fungal attack rate is the principal controllable parameter of biocontrol performance. These results highlight the importance of factors that sustain fungal activity, such as inoculum density, fungal persistence in soil, and environmental conditions.

Although simplified, the model provides a theoretical framework for exploring the dynamics of fungal-based biocontrol and may be adapted to other nematode–antagonist systems. Future developments incorporating environmental variability, spatial structure, an explicit egg stage, multi-species interactions, and damage functions that relate nematode density to yield loss may improve its predictive capacity. Model predictions can be tested experimentally by monitoring J2 density in soil, colony-forming units of *P. lilacinum*, egg-laying females or egg masses, parasitism of eggs and egg masses, and root fresh mass over time, together with soil temperature, moisture, and pH.

Overall, these findings support the potential of *P. lilacinum* as a component of sustainable nematode management and demonstrate the value of computational modeling as a complementary tool for generating hypotheses and guiding future empirical research.

## ACKNOWLEDGEMENTS

We thank the Instituto Federal Goiano (IF Goiano) and the Center of Excellence in Bioinputs (CEBIO) for institutional support and research infrastructure. We also acknowledge the administrative support provided by FUNAPE (Fundação de Apoio à Pesquisa) and the funding support from FAPEG (Fundação de Amparo à Pesquisa do Estado de Goiás) and FAPESC (Fundação de Amparo à Pesquisa e Inovação do Estado de Santa Catarina). The views and conclusions expressed in this article are those of the authors and do not necessarily reflect the official positions of the supporting institutions.

## CONFLICT OF INTEREST

We have no conflict of interest to declare.

## REFERENCES

Bird, A. F., & Kaloshian, I. (2003). Are roots special? Nematodes have their say. *Physiological and Molecular Plant Pathology*, 62(2), 115–123. https://doi.org/10.1016/S0885-5765(03)00045-6

Castagnone-Sereno, P., Danchin, E. G. J., Perfus-Barbeoch, L., & Abad, P. (2013). Diversity and evolution of root-knot nematodes, genus *Meloidogyne*: New insights from the genomic era. *Annual Review of Phytopathology*, 51, 203–220. https://doi.org/10.1146/annurev-phyto-082712-102300

Ciancio, A., Cabrera, I. M., Hidalgo-Díaz, L., Puertas, A., & Duvergel, Y. C. (2022). Modeling root-knot nematode regulation by the biocontrol fungus *Pochonia chlamydosporia*. *Frontiers in Fungal Biology*, 3, 900974. https://doi.org/10.3389/ffunb.2022.900974

Dahlin, P., Eder, R., Consoli, E., Krauss, J., & Kiewnick, S. (2019). Integrated control of *Meloidogyne incognita* in tomatoes using fluopyram and *Purpureocillium lilacinum* strain 251. *Crop Protection*, 124, 104874. https://doi.org/10.1016/j.cropro.2019.104874

Desaeger, J., Wram, C., & Zasada, I. (2020). New reduced-risk agricultural nematicides: Rationale and review. *Journal of Nematology*, 52, e2020-91. https://doi.org/10.21307/jofnem-2020-091

El-Ashry, R. M., Ali, M. A. S., Elsobki, A. E. A., & Aioub, A. A. (2021). Integrated management of *Meloidogyne incognita* on tomato using combinations of abamectin, *Purpureocillium lilacinum*, rhizobacteria, and botanicals compared with a nematicide. *Egyptian Journal of Biological Pest Control*, 31, 93. https://doi.org/10.1186/s41938-021-00438-x

Elling, A. A. (2013). Major emerging problems with minor *Meloidogyne* species. *Phytopathology*, 103(11), 1092–1102. https://doi.org/10.1094/PHYTO-01-13-0019-RVW

Gupta, R., Sharma, G. C., & Sharma, P. (2018). Life table of *Meloidogyne incognita* (southern root-knot nematode) on tomato. *Journal of Entomology and Zoology Studies*, 6(4), 251–256.

Hunt, D. J., & Handoo, Z. A. (2009). Taxonomy, identification and principal species. In R. N. Perry, M. Moens, & J. L. Starr (Eds.), *Root-knot nematodes* (pp. 55–97). CABI Publishing. https://doi.org/10.1079/9781845934927.0055

Jones, J. T., Haegeman, A., Danchin, E. G. J., Gaur, H. S., Helder, J., Jones, M. G. K., Kikuchi, T., Manzanilla-López, R., Palomares-Rius, J. E., Wesemael, W. M. L., & Perry, R. N. (2013). Top 10 plant-parasitic nematodes in molecular plant pathology. *Molecular Plant Pathology*, 14(9), 946–961. https://doi.org/10.1111/mpp.12057

Khan, M., & Tanaka, K. (2023). *Purpureocillium lilacinum* for plant growth promotion and biocontrol against root-knot nematodes infecting eggplant. *PLoS ONE*, 18(3), e0283550. https://doi.org/10.1371/journal.pone.0283550

Lu, C. J., Meng, Y., Wang, Y. L., Zhang, T., Yang, G. F., Mo, M. H., Ji, K. F., Liang, L. M., Zou, C. G., & Zhang, K. Q. (2022). Survival and infectivity of second-stage root-knot nematode *Meloidogyne incognita* juveniles depend on lysosome-mediated lipolysis. *Journal of Biological Chemistry*, 298(3), 101637. https://doi.org/10.1016/j.jbc.2022.101637

Machado, A. C. Z. (2014). Current nematode threats to Brazilian agriculture. *Current Agricultural Science and Technology*, 20(1), 26–35.

Moens, M., Perry, R. N., & Starr, J. L. (2009). *Meloidogyne* species: A diverse group of root-knot nematodes. In R. N. Perry, M. Moens, & J. L. Starr (Eds.), *Root-knot nematodes* (pp. 1–17). CABI Publishing. https://doi.org/10.1079/9781845934927.0001

Nicol, J. M., Turner, S. J., Coyne, D. L., den Nijs, L., Hockland, S., & Tahna Maafi, Z. (2011). Current nematode threats to world agriculture. In J. Jones, G. Gheysen, & C. Fenoll (Eds.), *Genomics and molecular genetics of plant–nematode interactions* (pp. 21–43). Springer, Dordrecht. https://doi.org/10.1007/978-94-007-0434-3_2

Noling, J. W. (2016). *Nematode management in tomatoes, peppers, and eggplant* (ENY-032). University of Florida, IFAS Extension.

Orion, D., & Kritzman, G. (1991). Antimicrobial activity of *Meloidogyne javanica* gelatinous matrix. *Revue de Nématologie*, 14(4), 481–483.

Parajuli, G., Kemerait, R., & Timper, P. (2014). Improving suppression of *Meloidogyne* spp. by *Purpureocillium lilacinum* strain 251. *Nematology*, 16(6), 711–719. https://doi.org/10.1163/15685411-00002799

Ploeg, A., & Maris, P. (1999). Effects of temperature on the duration of the life cycle of a *Meloidogyne incognita* population. *Nematology*, 1(4), 389–393. https://doi.org/10.1163/156854199508388

Santos, R. S., & Martinelli, P. R. P. (2022). Controle biológico de *Meloidogyne* spp. com fungos nematófagos em cultivo de cenoura. *Research, Society and Development*, 11(12), e157111234301. https://doi.org/10.33448/rsd-v11i12.34301

Seinhorst, J. W. (1965). The relation between nematode density and damage to plants. *Nematologica*, 11(1), 137–154. https://doi.org/10.1163/187529265X00582

Williamson, V. M., & Hussey, R. S. (1996). Nematode pathogenesis and resistance in plants. *The Plant Cell*, 8(10), 1735–1745. https://doi.org/10.1105/tpc.8.10.1735

*To cite this paper, use:*

Santos, D.V., Moreira, B.R., & Bernardes Neto, J.F. (2026). A tri-trophic model for the biological control of *Meloidogyne javanica* by *Purpureocillium lilacinum*: stability analysis and a biocontrol threshold. *Multi-Science Journal*, 9(2): 27-36. DOI: https://doi.org/10.33837/msj.v9i2.1824